INVESTIGATION OF THE MECHANICAL AND MICROSTRUCTURAL PROPERTIES OF WELDED API X70 PIPELINE STEEL

T. M. Ike, O. Adedipe, S. A. Lawal*, M. S. Abolarin and O. A. Olugboji

Department of Mechanical Engineering, Federal University of Technology, Minna, Nigeria

*Corresponding author's e-mail address: lawalsunday@futminna.edu.ng

ARTICLE INFORMATION

ABSTRACT

The mechanical properties of pipelines particularly those in marine environments are influenced by corrosion activity of seawater throughout their service lives. The degree to which these properties are influenced in seawater compared to those exposed to air needs to be better understood. In this study, the chemical composition of API X70 pipeline steel plate, microstructure and mechanical properties of the welded joints of same steel plates exposed to ambient air and seawater respectively were investigated. It was found that the base metal consisted of manganese (0.51wt% Mn), low carbon content (0.051 wt% C) and small quantities of alloying elements such as vanadium (0.021wt% V), molybdenum (0.118 wt% Mo), chromium (0.240 wt% Cr), copper (0.002 wt% Cu), and a carbon equivalent (CE IIW) of 0.38. Scanning Electron Microscope (SEM) showed that the microstructure of base metal sample has large grains formed in packets which have certain crystallographic orientation but contain submicron grains arranged in a chaotic interlocking manner. The tensile tests performed using a UNITED type universal testing machine confirmed that the yield strength of the base metal was 573.045MPa which conforms to API standard for X70 steel pipe. The manual metal arc (MMA) welding technique was applied to produce the welded joints. For the welded joints exposed to ambient air at room temperature, the yield strength was 680.624MPa while the compressive strength was 1500.2MPa, and the impact energy at -10°C was 112.68J. Air tests referred to tests conducted in the laboratory at room temperature. For the welded joints exposed to seawater for 12 weeks, the yield strength was 609.154MPa while the compressive strength was 1219.34MPa, and the impact energy at -10°C was 61.48J. The above results for air and seawater exposures were used to determine the environmental reduction factors of the two environments. Hardness tests conducted using Vickers hardness tester revealed variations in hardness across the base metal, the HAZ and the weld, with the weld having the highest average Vicker's hardness value (223.8HV) followed by the base metal (217.3HV) and the HAZ had the least (214.5HV)

1.0   Introduction

In various service environments, pipelines used for the transport of natural resources including oil and gas present an enormous challenge as the failure of the pipeline is always associated with serious environmental damage and heavy losses (Hopkins, 2007). Most often, the failure

starts at welded joints that join different elements of pipeline steel (Nanninga et al., 2010). The pipeline industry has shown an increasing demand for pipeline steel that can transport diverse and higher quantities of petroleum products at higher operating pressures across hostile (marine) environments and this has led to the use of higher strength steel grades (Fabian et al., 2010). Current pipeline materials in the world market are often regulated according the American Petroleum Institute's (API) standard 5L. The main design considerations outlined in API-5L are based on alloy chemistry and tensile strength. The chemical compositions of the X-grade steels are such that there are maximum limits on C, Mn, S, P in combination with dispersoid-forming elements such as niobium and vanadium (Omale et al., 2017). The variations in strength (for example, between X70 and X80) do not result primarily from variations in alloy composition, but from variations in the processing route of the steel (Omale et al., 2017). TM processing allows the yield strength of the pipe steels to be tailored through combinations of grain refinement, precipitation hardening (micro-alloying) and phase formation (Cheng and Xue, 2011). The risk associated with pipeline in terms of safety of people, damage to the environment and loss of income has been a major concern to pipeline integrity managers. There have been a number of studies conducted by researchers on causes of oil pipeline failures in the oil and gas industry.

Nakano et al. (1993) examined the corrosion fatigue crack propagation behavior of welded carbon steels and demonstrated that crack propagation rates can be higher in hardened weld area microstructures than the parent material. Omale et al. (2017) studied the microstructure and mechanical properties of welds in pipeline steel and discovered that hardness was highest in the weld bead, a bit lower in the base metal and lowest in the heat affected zone. In this study, higher density of voids was observed at the top of the weld bead than in the middle. It was also demonstrated that large grains and dislocation density in heat affected zone is related to the high susceptibility of the steel weld to failure under tensile load. Aliu (2012) investigated the mechanical and microstructural properties of welded joint of Nigerian National Petroleum Corporation pipelines and observed that the pipeline was made of high strength low alloy (HSLA-A105) steel. At the end of the investigations, it was concluded that inadequate mechanical tests and lack of micro structural examination of the welded joints before installations were possible sources of pipeline failures.

Omale et al. (2017) studied the evolution of microstructure, texture and mechanical properties of API X70 pipeline steel after different thermomechanical treatments using a combination of X-ray diffraction and electron backscatter diffraction (EBSD). The investigations revealed that different microstructure consisting of polygonal ferrite, bainite, coarse and fine acicular ferrite grains was obtained with a centre line segregation traversing through and parallel to the rolling direction. EBSD investigations confirmed that both dynamic recovery and partial recrystallization occurred during hot rolling requiring further annealing for a more homogenous equiaxied grain structure. It was also observed that after accelerated cooling, the fast cooling rate and low temperature interruption allows the formation of more bainite which in turn increased the tensile strength of the steel.

Leonardo et al. (2014) investigated the microstructure and mechanical properties of two API steels for iron ore pipelines. A chemical analysis of X70 steel was performed by means of a ThermoARL optical emission spectrometer and the microstructure was observed by a JEOL scanning electron microscope (SEM). The chemical composition of the X70 steel used for the experimental investigation in Leonardo et al. (2014) is shown in Table 1.

Corresponding author's e-mail address: lawalsunday@futminna.edu.ng

Table 1: Chemical composition of API-5L X70 steel (wt%)

C	Si	S	P	Mn	Ni	Cr	Cu	Al	Ti	Nb	V
0.109	0.239	0.004	0.023	1.536	0.011	0.024	0.011	0.026	0.016	0.045	0.045

Source: Leonardo et al. (2014)

The tensile, impact and hardness tests revealed yield strength of 586MPa, tensile ultimate strength of 640MPa, a total elongation of 38%, Rockwell hardness A, HRA 65, and Charpy impact absorbed energy of 184J (Leonardo et al. 2014). However, in this study, the mechanical properties of welds exposed to ambient air and welds exposed to seawater were investigated as a means of estimating the environmental reduction factors. In this paper, mechanical tests were conducted on samples that are extracted from API X70 pipeline steel. Results are presented for tests conducted in air at room temperature and are compared with results obtained from samples that are exposed to seawater, in order to have a better understanding of the influence of time dependent activity of corrosion on mechanical properties of steel.

2.0   Materials and Methods

2.1   Materials

API X70 pipeline steel plates of thickness 20.8mm with equal width and length of 304.8mm was used as the base metal or test specimen. This material was obtained from the engineering laboratory of the Pipe Construction Company belonging to SCC Nig Ltd at Ushafa, Bwari, Abuja FCT-Nigeria. The seawater used for testing was obtained from Lagos lagoon.

2.2   Methods

The first task carried out in order to prepare the steel plate for welding was the removal of all the impurities such as rust and oxide by cleaning the edges using iron brush. A butt joint was prepared by using cutting technique and a double V joint preparation was adopted to make for easier welding with less metal weld and less distortion. The manual metal arc (MMA) welding technique, in flat welding positions (1G), was applied to fill the joints. A sketch of the typical joint prepared before the welding is as shown in Figure 1.
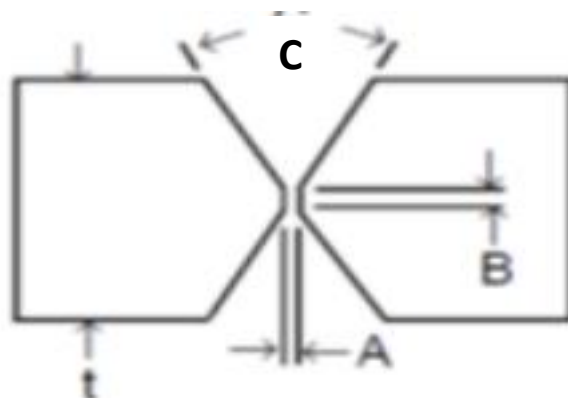

Figure 1: Diagram of weld joint prepared before welding specimen plates

where: t (plate thickness) = 20.8mm, A (Root opening) = 4mm, B (land thickness) = 2.4mm and C (groove angle) = 60°

Welding joints were produced using manual metal arc (MMA) welding technique. This method was the recommended and established method used by the operators of the SCC Abuja test

facility. To ensure conformity to the American Society for Testing and Materials (ASTM) D114 on standard composition of seawater, the seawater was tested and analysed at the Chemistry lab in River Basin office, Minna, Niger State. A total of ten (10) tensile test specimens with welded joints were prepared, five of them were immersed into seawater, while the remaining five were exposed to ambient air. Ambient air refers to the normal laboratory condition. For the compressive tests using the universal testing machine located in SCC Abuja, ten (10) test specimens with welded joint were also prepared; five of the specimens were immersed into the seawater, while the other five were exposed to ambient air. Hardness test was also conducted using the Vickers hardness tester located in SCC Abuja. The tests were conducted in accordance with the specifications in API 5L standard. Hardness test was conducted on specimen containing sections of the base metal, heat affected zone (HAZ) and weld. It was ensured that the specimen was extracted in a way to encompass the weld, base material and the HAZ of the plate. In order to reveal the location of the HAZ, a slice extracted from the weld area was etched by applying 2 % Nital solution. The Toughness of the welds was investigated at SCC Abuja using the Charpy method and based on the specifications in ISO 148 standard. Ten (10) Charpy test specimens with welded joints were also prepared and likewise, five of the specimens were immersed into seawater while the rest were exposed to ambient air. The duration for the immersion into seawater for all test specimens was 12 weeks after which tensile, compressive and Charpy tests were conducted. The choice of the immersion time was based on the investigators decision bearing in mind that the phenomenon of corrosion will be revealed regardless of the soaking or immersion period. At this juncture, it should be mentioned that corrosion damage is time dependent. It should therefore be expected that in simulated corrosive environment used during experimental investigation, the effect on corrosion will be revealed regardless of soaking time. Microstructural examination and analysis of fracture surfaces of the samples were carried out using the scanning electron microscope (SEM) located at Spectral Research and Laboratory Kaduna, while spectroscopic analysis was carried out at Oshogbo machine tools. Figures 1 to 4 show the pictures of test specimens used while Figures 5-8 are the corresponding schematic representations.

Figure 1: Tensile test specimen

Corresponding author's e-mail address: lawalsunday@futminna.edu.ng

Figure 2: Compressive test specimen

Figure 3: Charpy test specimen

Figure 4: Hardness test specimen
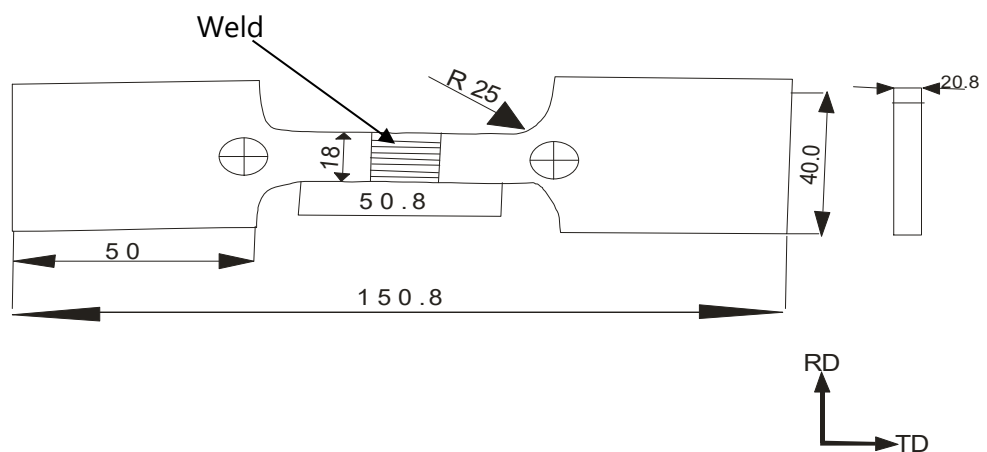
Figure 5: Schematic of the tensile test specimen with welded joint

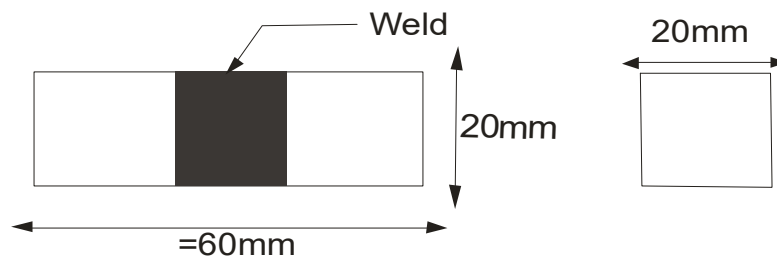*Corresponding author's e-mail address: lawalsunday@futminna.edu.ng*

Figure 6: Schematic of the compressive test specimen with welded joint
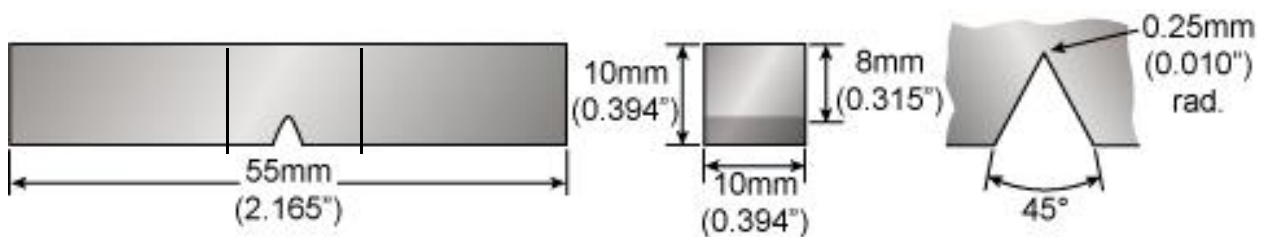
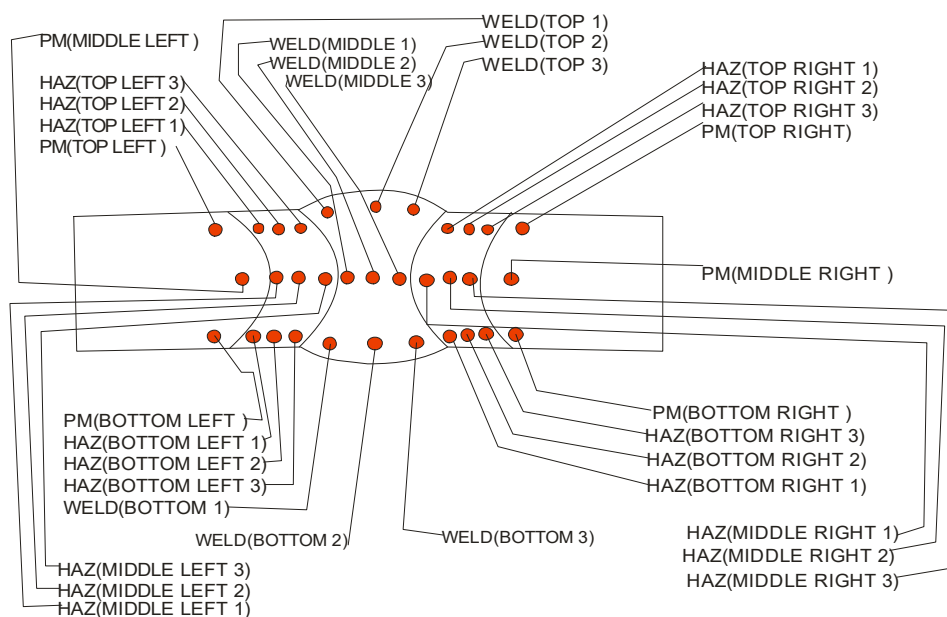Figure 7: Schematic for Charpy-V notch specimen

Figure 8: Schematic of hardness test specimen showing the various points of indentation

3. Results and Discussions

The following sections present the results of microstructure, chemical properties of the steel that was used for investigation as well as the results and discussions of the mechanical tests such as tensile, compressive toughness and hardness tests.

3.1 Microstructure of Base metal

The micrograph obtained from base material through SEM is shown in Figure 9 where large grain sizes can be observed, and this depicts ductility. Basically, ductility is caused by the slip phenomenon of crystals and slip lines are confined to the grain boundaries. The finer the grain

Corresponding author's e-mail address: lawalsunday@futminna.edu.ng

sizes may be related to the lesser ductility. However, in case of larger grains, larger amounts of slip could occur thus, giving better ductility (Morris, 2013).
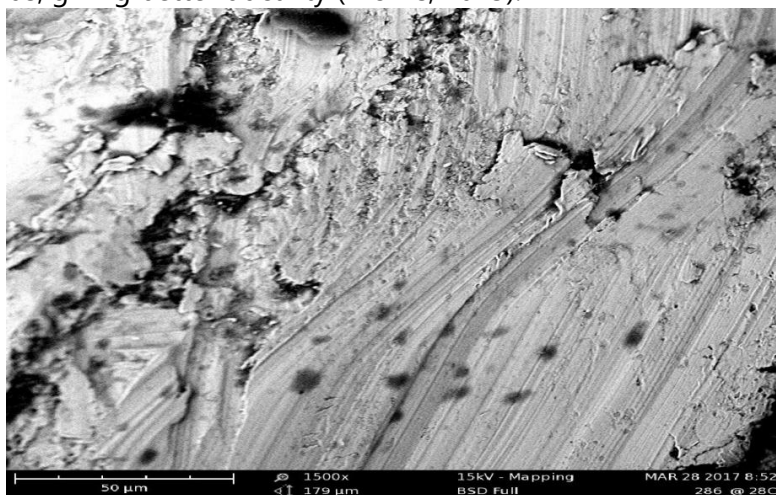

Figure 9: Microstructure of base metal in air (1,500X)

3.2 Chemical Composition of Base Metal

Spectroscopic analysis involves the dispersion of an object's light into its component colors (i.e. energies). By performing this dissection and analysis of an object's light, one can infer the physical properties of that object (such as temperature, mass, luminosity and composition). Table 2 contains the chemical composition and CE of the base metal after the spectroscopic analysis was conducted.

Table 2: Chemical composition of sample base metal

Elements	%C	%Si	%Mn	%Cr	%Mo	%Ni	%V	%Cu	%Al	CE (IIW)
Base metal	0.051	0.210	1.510	0.240	0.118	0.071	0.021	<0.002	0.048	0.38

3.3 Seawater Analysis

The laboratory analysis of the seawater put the pH level at 7.8 and showed that the percentage composition of the seawater as: Sodium Chloride (NaCl) was 58%, Magnesium Chloride ($MgCl_2$) was 26%, Sodium Sulfate $NaSO_4$ was approximately 10%. Other salts present in small amounts include calcium chloride (2.4%), potassium chloride (1.3%), sodium bicarbonate (0.5%), and sodium fluoride (0.007%). The values are in agreement with the ASTM D1141 standard for the preparation of substitute seawater.

3.5 Tensile Strength

Five tensile test results for welded joints exposed to air and seawater respectively were recorded and plotted as shown on Figure 10. It was observed that the tensile strength of the welds reduced after exposure to seawater environment for 12 weeks. The average tensile strength of the samples that were exposed to seawater was found to be 609.154 MPa, while for those exposed to air was 680.624 MPa. The percentage reduction in tensile strength was found to be 10.5%, which implies that the corrosive activity of the seawater would be revealed irrespective of the exposure time as mentioned previously. However, it must be mentioned that investigation of mechanical properties of the unwelded samples is beyond the scope of this paper.
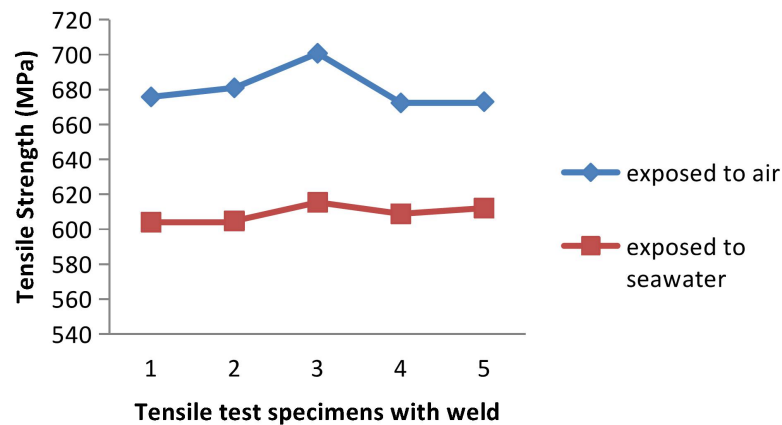
Figure 10: Tensile strength for tensile test specimens with weld joints

3.6 Compressive

Figure 11 shows that the compressive strength of all five compressive test samples with welded joint were reduced after immersion into seawater environment for 12 weeks. The average compressive strength of the samples exposed to seawater was 1209.34 MPa, while those exposed to air was found to be 280.68 MPa. The percentage reduction in compressive strength was determined to be 18.7%, which implies that the effect of soaking time was significant in compressive test samples than in samples used for tensile tests.
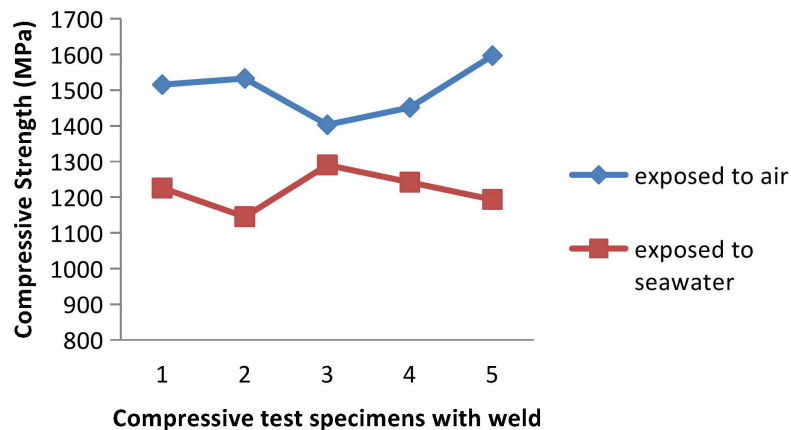

Figure 11: Compressive strength for compressive test specimens with weld joints

3.7 Hardness

The hardness test results are shown on Table 3 while Figure 12 depicted the hardness profile across the weld top surface. From Table 3 the Weld has a higher average hardness value of 223.8 HV compare to HAZ which has an average value of 214.5 HV as well as the parent metal with an average value of 217.3 HV. These results obtained are in agreement with the work done by Omale et al. (2017). The variations in the hardness across the weld may be attributed to several factors such as residual stresses developed just after welding. From the microstructural point of view, the high hardness in the weld may be attributed to the fine grain size, and the interlocking

Corresponding author's e-mail address: lawalsunday@futminna.edu.ng

nature of the ferrite grains (Loureiro, 2002). One of the factors contributing to lower hardness in the HAZ is high heat input below its melting point and hence retention of heat in this region. The lower hardness in the HAZ might be explained by the intense grain growth in this region resulting from high heat input below its melting point (Kacar and KöKemli, 2005)

Table 3: Vickers's hardness values

| S/N	Part	HV	S/N	Part	HV
1	PM top left	217	18	HAZ top right 3	230
2	PM top right	220	19	HAZ middle right 1	224
3	PM middle right	221	20	HAZ middle right 2	220
4	PM middle left	219	21	HAZ middle right 3	229
5	PM bottom left	214	22	HAZ middle left 1	229
6	PM bottom right	213	23	HAZ middle left 2	199
7	HAZ top left 1	218	24	HAZ middle left 3	208
8	HAZ top left 2	206	25	HAZ bottom left 1	217
9	HAZ top left 3	219	26	HAZ bottom left 2	204
10	HAZ top right 1	220	27	HAZ bottom left 3	205
11	HAZ top right 2	205	28	HAZ bottom right 1	234
12	HAZ bottom right 2	200	29	Weld middle 2	224
13	HAZ bottom right 3	195	30	Weld middle 3	232
14	Weld top 1	218	31	Weld bottom 1	231
15	Weld top 2	202	32	Weld bottom 2	238
16	Weld top 3	213	33	Weld bottom 3	232
17	Weld middle 1	224			
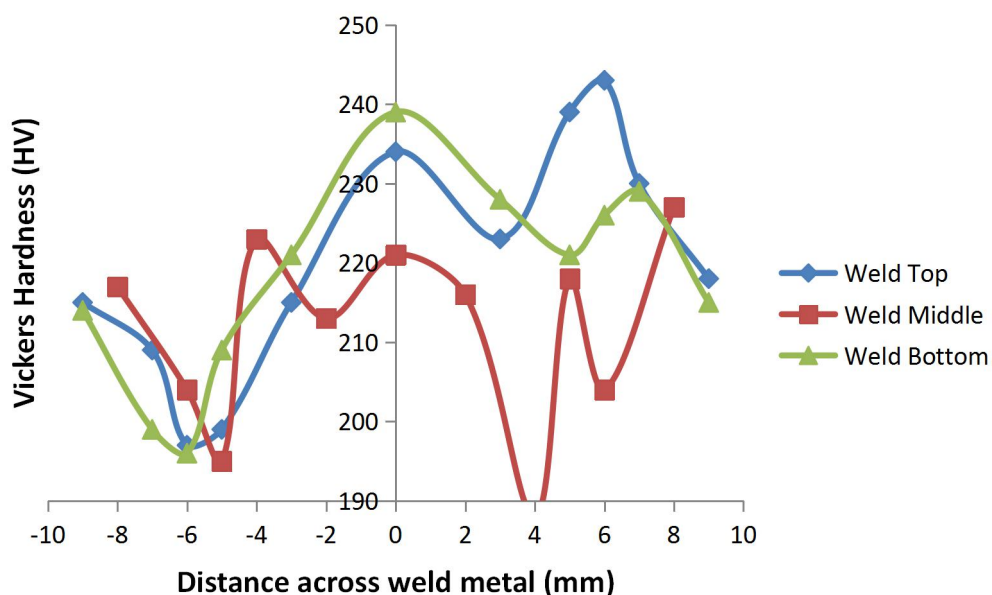
Figure 12: Hardness profile as a function distance from the center of weld bead

3.8 Charpy

The test results are shown in Table 4 and represented in Figure 13, it can be observed that the impact energy of the weld samples exposed to air is higher than the impact energy of the weld samples exposed to sea water at all the temperatures used. The lower impact energy observed for weld samples exposed to seawater was due to the corrosive environment which affected the microstructure of the weld. The test results also confirm the work done by Nakano et al, (1993), concerning corrosion fatigue crack propagation behaviour of TMCP steels.

Table 4: Charpy impact test result

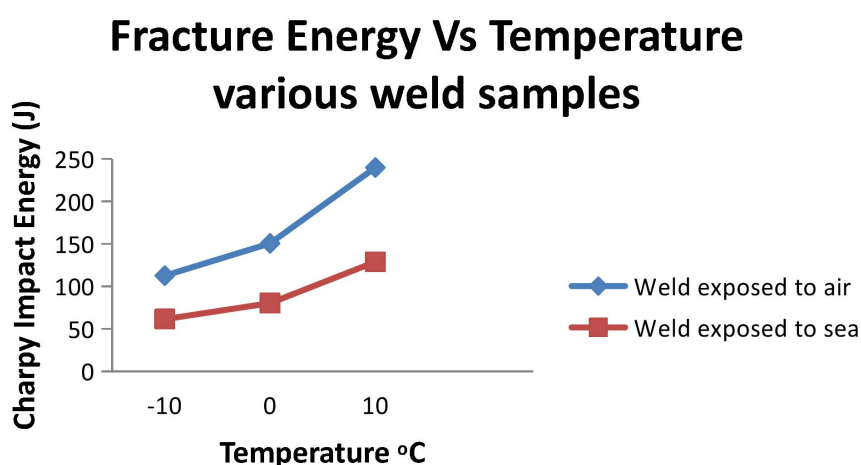| Type of experiment	Energy (J) at impact at -10°C	Energy (J) at impact at 0°C	Energy (J) at impact at 10°C
Test Sample exposed to ambient air	112.68	150.7	240.8
Test Sample exposed to seawater	61.48	80.3	150.7

Figure 13: Fracture energy (J) and Temperature (°C)

3.9 Fracture Surfaces of Charpy Test Specimen

Figures 14(a-b) show SEM images of the fracture surfaces of X70 steel Charpy test specimens with welded joints. The fracture surface morphology of the specimen without exposure to corrosive environment was 100% ductile with numerous fine dimples in the fracture surface which is considered a sign of ductile fracture as shown in Figure 14a. Moreover, a considerable amount of necking was observed during deformation. After exposure to seawater for three months the fracture surface was still predominantly ductile and shows evidence of dimples. This specimen also shows some necking during deformation as shown in Figure 14b. It means that if the specimen were exposed for a longer time, it would eventually show the characteristics of completely brittle failure.

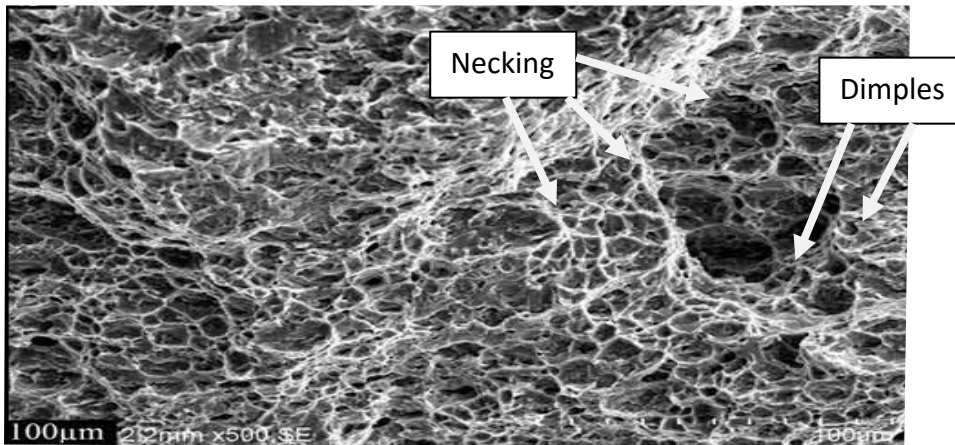*Corresponding author's e-mail address: lawalsunday@futminna.edu.ng*

Figure 14a: SEM images of the fracture surfaces of weld Charpy test specimen
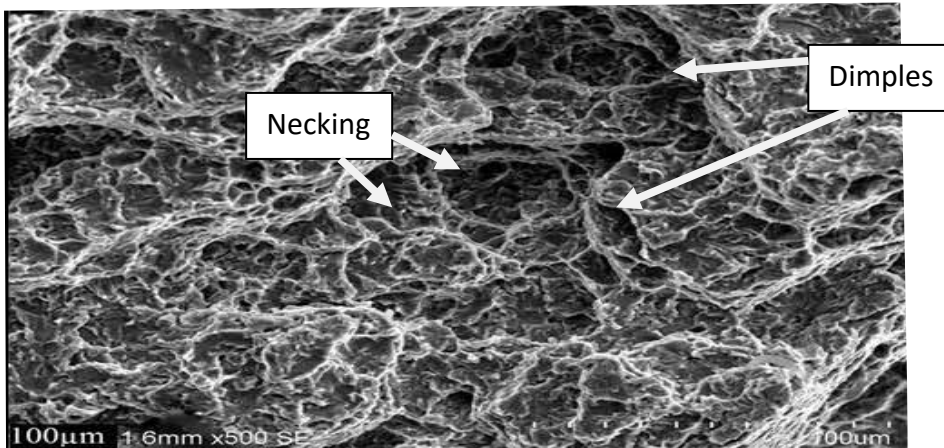

Figure 14b: SEM images of the fracture surfaces of weld Charpy test specimen exposed to seawater for 12 weeks.

4.0 Conclusions

Based on the characterization of structure carried out with SEM, Spectroscopic analysis, and investigation of mechanical properties through destructive testing experiments, the following conclusions may be drawn.

1. Large grain sizes were observed in the microstructure of the sample API X70 steel plate and that implied that the steel was ductile since large grains give room for large amounts of slip to occur thus giving better ductility. The API X70 steel base metal composed of manganese (0.51wt% Mn), iron (97.73 wt% Fe), in combination with very low carbon content (0.051 wt% C) and minor additions of alloying elements such as vanadium (0.021wt% V), molybdenum (0.118 wt% Mo), chromium (0.240 wt% Cr), copper (0.002 wt% Cu), and a carbon equivalent (CE IIW) of 0.38. The API X70 is therefore classified as low carbon steel with alloying elements (Mn, V, Cr, Si, Ni, Mo and Cu) that help in the strengthening of the ferrite

2. The average tensile strengths for welded joints exposed to air and seawater for 12 weeks were 680.624MPa and 609.154MPa respectively while the average compressive strengths for welded joints exposed to air and seawater for 12 weeks were 1500.02MPa and 150.75MPa respectively. At the temperature of zero degrees Celsius and same exposure period, the Charpy impact energy absorbed by welded joint exposed to air was 150.7J while that absorbed by welded joints exposed to seawater was 80.3J.

3. The hardness profile of welded joints showed variations in hardness across the base metal, HAZ and weld metal whereby the weld metal had the highest value of hardness (223.8HV) followed by the base metal (217.3HV) and the HAZ had the least (214.5HV).

4. The mechanical properties of the welds are compromised by exposure to corrosive environment such as seawater as observed in the results obtained from tensile, compressive, and Charpy test experiments. The results showed 10.5% reduction in the tensile strength, 18.7% reduction in compressive strength and at least 37% decrease in impact energy absorbed by the welds after exposure to seawater for 12 weeks.

References

Aliu, S. 2012. Investigation of mechanical and microstructural properties of welded joint of Nigerian National Petroleum Corporation pipelines. M. Eng. Thesis, Federal University of Technology Minna, Nigeria.

Cheng, YF. and Xue, HB. 2011. Characterization of inclusion of X80 pipeline steel and its correlation with hydrogen-induced cracking. Corrosion Science, 53(4): 1201-1208.

Fabian, G., Heike, M., Florian, G. and Elke M. 2010. Super-High Strength Steel. 2nd International conference on Super-High Strength Steel, Peschiera Del Garda, Italy, 17th to 20th October 2010, (www.tib.eu)

Hopkins, P. 2007. Pipeline stream, past, present, and future' from the 5th Asian Pacific IIW international congress. Sydney, Australia.

Kacar, R, and KöKemli, K 2005. Effect of controlled atmosphere on the MIG -MAG arc weldment properties. Materials & Design, 26(6): 508-516.

Leonardo BG., Luiz CC., Rodrigo VB. and Soares, LH. 2014. Microstructure and mechanical properties of two API steels for Iron ore pipelines. Journal of Universidade federal de ouropreto, MG, Brazil, 17: 1516 – 1639.

Loureiro , AJ. 2002. Effect of heat input on plastic deformation of undermatched welds. Journal of Materials Processing Technology. 128(1): 240-249.

Morris, JW. Jr. 2013. The Influence of Grain Size on the Mechanical Properties of Steel. Department of Materials Science and Engineering, University of California, Berkeley and Center for Advanced Materials, Lawrence Berkeley Laboratory, Berkeley, CA 94720.

Nakano, Y., Matsumoto, S., Watanabe, O. and Hatomura, T. 1993. Corrosion fatigue crack propagation behaviour of TMCP Steel. Offshore Mechanics and Arctic Engineering, - Pipeline Technology, 5: 215-223.

Nanninga, N., Slifa, A., Levy, L. and hite, C. 2010. A Review of fatigue crack growth for pipeline steel exposed to Hydrogen" Journal of Reserve National Institution Standard Technology, 115 (6): 437-452.

Omale JI., Oheri, EG., Tiamiyu, AA., Eskandari, M. and Szpunar, JA. 2017. Microstructure, texture evolution and mechanical properties of X70 pipeline steel after different thermo mechanical treatments. Material Science and Engineering, 703: 497 – 485.

Corresponding author's e-mail address: lawalsunday@futminna.edu.ng

Nomenclature:

HAZ	Heat Affected Zone
API	American Petroleum Institute
IIW	International Institute of Welding
ASTM	American Standards for Testing Materials
AWS	American Welding Society
SEM	Scanning Electron Microscope
EBSD	Electron Back Scattered Diffraction
DWTT	Drop Weight Tear Test
TEM	Transmission Electron Microscope
SAW	Submerged Arc Welding
MMA	Manual Metal Arc welding
TMCP	Thermo Mechanically Controlled Processing
HV	Vickers Hardness number
CE	Carbon Equivalent
OD	Outside Diameter
BM	Base Metal
FZ	Fusion Zone
N	Newton
X70	Graded steel specification
wt	Weight
oC	Degree Celsius
α	Alfa particle
γ	Gamma particle
μm	Micrometer
MPa	Mega Pascal
Kg/L	kilogram per litre
g/L	gram per litre
N/mm^2	Newton per millimeter square